Impacts of large-scale land-use change on the uptake of polycyclic aromatic hydrocarbons in the artificial Three…

Article · November 2016

DOI: 10.1021/acs.est.6b04835

CITATION
1

READS
64

10 authors, including:

Tao Huang
Lanzhou University
30 PUBLICATIONS **119** CITATIONS
SEE PROFILE

Hong Gao
China Medical University (PRC)
170 PUBLICATIONS **1,512** CITATIONS
SEE PROFILE

Chongguo Tian
Chinese Academy of Sciences
82 PUBLICATIONS **624** CITATIONS
SEE PROFILE

Jianmin Ma
Lanzhou University
105 PUBLICATIONS **1,907** CITATIONS
SEE PROFILE

Environmental Science & Technology

Article

pubs.acs.org/est

Impacts of Large-Scale Land-Use Change on the Uptake of Polycyclic Aromatic Hydrocarbons in the Artificial Three Northern Regions Shelter Forest Across Northern China

Tao Huang,[†] Xiaodong Zhang,[†] Zaili Ling,[†] Leiming Zhang,[‡] Hong Gao,[†] Chongguo Tian,[§] Jiujiu Guo,[†] Yuan Zhao,[†] Li Wang,[†] and Jianmin Ma*[,†,∥]

[†]Key Laboratory for Environmental Pollution Prediction and Control, Gansu Province, College of Earth and Environmental Sciences, Lanzhou University, Lanzhou 730000, P. R. China

[‡]Air Quality Research Division, Environment and Climate Change Canada, Ontario M3H 5T4, Canada

[§]Key Laboratory of Coastal Zone Environmental Processes and Ecological Remediation, Yantai Institute of Coastal Zone Research, Chinese Academy of Sciences, Yantai 264003, China

[∥]CAS Center for Excellence in Tibetan Plateau Earth Sciences, Beijing 100101, China

Supporting Information

ABSTRACT: This study quantifies the influence of large-scale land-use change induced by the artificial Three-Northern Regions Shelter Forest (TNRSF) across northern China on the environmental cycling of organic chemicals. Atmospheric removal and long-term trends of two polycyclic aromatic hydrocarbon (PAH) species, phenanthrene (PHE) and benzo[*a*]pyrene (BaP), resulting from increasing vegetation coverage and soil organic carbon in the TNRSF over the last two decades were examined. Field sampling data and modeling result showed that the total atmospheric removal of PHE by TNRSF increased from 36.4 tons in 1990 to 76.8 tons in 2010, increasing at a rate of 5.6% yr^{-1}, and BaP from 2.2 to 4.5 tons, increasing at a rate of 5.2% yr^{-1}. Three model scenarios were designed to distinguish the effects of atmospheric emissions, and with and without TNRSF on the environmental fate of PAHs. Approximately 1−4% of PHE and BaP emitted in northern China were removed by the TNRSF during 1990−2010. Model simulations revealed that the TNRSF enhanced atmospheric removal of PHE by 29% and BaP by 53% compared with the simulation without the TNRSF, manifesting marked contributions of land-use change by the artificial TNRSF, the largest afforestation activity in human history, to the atmospheric removal of organic chemicals.

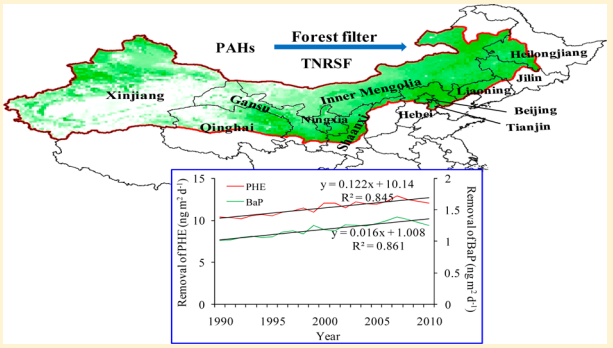

1. INTRODUCTION

Human activities significantly impact the biogeochemical cycling of organic chemicals (OCs), including persistent organic pollutants (POPs) and POP-like chemicals, such as polycyclic aromatic hydrocarbons (PAHs),[1] through climate and land-use change. Extensive research on the interactions between climate change and OCs environmental cycling has been conducted in the past decade.[2−6] Komprda et al.[7] assessed the influence of temperature and land-use changes on the reemission of OCs from background and agricultural soils and showed that land-use change may significantly affect trends of atmospheric OCs. However, their investigation was based on a small area and projected land-use changes. The long-term environmental effects of OCs induced by large-scale land-use changes has not yet been investigated since land-use changes by human activities are often not readily linked with the biogeochemical cycling of OCs.

The Three Northern Regions Shelter Forest (TNRSF) program, also known as the Great Green Wall, was initiated in 1978 with the aims of preventing and slowing soil and water erosion in northern China. The TNRSF program is the largest ecosystem restoration project in the world and in human history. The project extends from 1978 to 2050 and was designated to cover a total area of 4.1 million km^2 (42.7% of the land area in China) (Figure S1). However, many land areas in the TNRSF region are not presently covered by forests, especially in many places in northwestern China where shrubs, instead of trees, are major vegetation types. By the end of the fourth phase of the TNRSF program (2010), the forest coverage in this region had increased from 5% in 1978 to

Received: September 23, 2016
Revised: November 3, 2016
Accepted: November 5, 2016
Published: November 5, 2016

DOI: 10.1021/acs.est.6b04835
Environ. Sci. Technol. XXXX, XXX, XXX−XXX

12.4%, leading to a significant artificial land-use change in northern China.[8−10] While the TNRSF aims to improve regional ecological environments,[11−15] it was recently found to play a role in the removal of sulfur dioxide (SO_2) and nitrogen oxide (NO_x) through dry deposition.[16] It was shown that the increasing vegetation coverage in the TNRSF over the past 30 years had increased its efficiency in removing air contaminations from the atmosphere. Compared with criteria air pollutants such as SO_2 and NO_x, the pathways in the uptake of organic pollutants by forests are more complex because they involve air−canopy exchange, air−soil exchange subjected to the soil organic carbon (SOC) content, and soil−vegetation exchange.

Since organic chemicals tend to partition from gas and liquid phases to organic phases,[17] the spatial distribution of atmospheric OCs is often driven by the gradient of organic carbon content in soils. The strong association of OCs with organic carbon pools in soils is therefore often taken into account when assessing the environmental fate of OCs. Forests have been identified as a very important terrestrial storage compartment for OCs because soils in equilibrium with forest ecosystems have a high carbon density.[17−24] Large surface roughness and leaf area index (LAI) of forests can also lead to rapid uptakes of OCs in forest canopies, there by reducing air pollutants levels through increasing deposition to forest leaves and underlying floors.[25−29] Matzner showed that bulk deposition of PAHs could be elevated under forest canopies.[27] Simonich and Hites estimated that 44% of the PAHs emitted from the northeast United States (US) were deposited into forests.[29] McLachlan and Horstmann linked the uptake of OCs by forests with a '"forest filter effect"', defined as the forest filtering airborne OCs from the atmosphere and transferring them to soil. They reported that annually averaged deposition of an organic chemical to forested soils was approximately a factor of 3−5 greater than that to bare soils.[28] Abundant observational evidence has revealed higher concentrations of OCs in forest soils than nearby treeless soils.[24,29−31] However, almost all previous studies in the associations between OCs environmental cycling and forests canopies were conducted in natural forests under a steady state[32] and have no significant changes in leaf area, SOC, and forest biomass for a long-term period. Since increasing forest biomass and carbon storage across China has been largely attributed to artificial forestation,[33−36] the significant land-use change induced by the TNRSF provide a unique opportunity to elucidate the impact of large scale artificial land-use change on the environmental fate of OCs. It is interesting to know how and to what extent the TNRSF would alter the cycling of OCs in the terrestrial environment. This will also contribute to our understanding of the interactions between human induced land-use changes and the biogeochemical cycle of organic pollutants.

In this study, two PAHs congeners, phenanthrene (PHE) and benzo[*a*]pyrene (BaP), were selected to investigate the impact of the TNRSF on the uptake of OCs from the atmosphere. Given their POP-like properties, PAHs have been categorized as POPs by the European Environment Agency and the Convention on Long-Range Transboundary Air Pollution Protocol.[1] PHE is primarily in gas phase and BaP is mostly particle-bound, which enables us to separately elucidate the influence of the TNRSF on the environmental cycling of gas-phase and particle-bound OCs. Field monitoring evidence for the uptake of PHE and BaP and changes in SOC by the TNRSF was first provided. A modified high-resolution atmospheric transport model was then applied to simulate PAHs removal in the TNRSF. Our study aims to measure the interactions between artificial large-scale land use change and the environmental fate of atmospheric contaminants through (1) assessing the potential contribution and significance of large-scale land-use change by artificial forests to the removal of OCs from the atmosphere, (2) quantifying the roles of the TNRSF in the depletion of OCs in a man-made large-scale forest, and (3) examining the long-term trend of the depletion of OCs in northern China resulting from the TNRSF development in the past 20 years and future.

2. METHODOLOGY

2.1. In Situ Field Measurement. A field campaign was conducted to measure the organic carbon content and soil concentrations of PAHs at several sites in the TNRSF to examine soil absorption of PAHs in the artificial forest and verify the SOC calculated by the satellite retrieved LAI. These sites are located in the Central-North region of the TNRSF near Beijing and Tianjin, the two megacities in northern China (Figures S1 and S2). Soil samples were collected at 4 paired sampling sites (4 inside forests and the other 4 outside forests) during August 7−12, 2015. The sampling sites, samples collections, laboratory processing and chemical analysis can be found in the Supporting Information (SI) (section SI2, Figure S2, and Table S1).

2.2. Atmospheric Transport Modeling. An atmospheric transport model (CanMETOP, Canadian Model for Environmental Transport of Organochlorine Pesticides)[37] was used to simulate long-term (1990−2010) trends of PHE and BaP in multiple environmental compartments. The major features of the model are the same as the global version of CanMETOP;[38] however, the horizontal spatial resolution is increased to 1/4° latitude by 1/4° longitude with 14 vertical levels. The CanMETOP considers the three-dimensional atmospheric advectiosn, eddy diffusion, dry/wet deposition, and degradation in air and soil. Modifications of the model in this study include coupling a fugacity based Level IV multimedia fate and transport module[37] for simulating OCs in soils and air-soil exchange processes, updating several trans-media or mass exchange processes and incorporating air-forest-soil exchange processes. The model domain covers the TNRSF and the surrounding regions (Figure S3). The annual gridded emission inventories of PHE and BaP across the model domain from 1990 to 2010 were established according to Zhang and Tao.[39] (Figures S3 and S4). Although fine particles of PAHs can be transported globally,[40] this study did not account for the influence of external PAH sources from other countries in their budget in northern China via long-range transport. Since China has been the largest PAH emission source worldwide,[39] local emissions dominated the environmental fate of PAHs. The model parametrization and uncertainty analysis are provided in SI (sections SI3−SI7). In the literature, model evaluations have been carried out by comparisons between the modeled and measured air concentrations in the model domain. Details of the model evaluation are presented in SI (section SI6). Overall, the results show that the modeled air concentrations agree with the sampled data at $r > 0.8$ ($p < 0.01$), indicating the reliability of the emission inventories and the CanMETOP model applied in the present study.

Three model scenarios are established to investigate the impacts of large-scale land-use changes by the TNRSF on the

DOI: 10.1021/acs.est.6b04835
Environ. Sci. Technol. XXXX, XXX, XXX−XXX

removal of PAHs from the atmosphere. The first scenario (model Scenario 1) implements the fixed emission of the two PAHs congeners by averaging their respective annual emissions from 1990 to 2010, and annually varying LAI and SOC from 1990 to 2010. This scenario is designed to eliminate the influence of the PAH primary emissions, which could otherwise overwhelm the environmental levels of PAHs, on the atmospheric removal of PAHs by the TNRSF. The second scenario (model Scenario 2) uses annually varying PAHs emission, LAI and SOC from 1990 to 2010 which is designed to compare with the results from the model Scenario 1 to distinguish the effects from emission and forest expansion on PAH environmental cycling. The third scenario (model Scenario 3) uses the annually varying emission of PAHs from 1990 and 2010 but fixed LAI and SOC values in 1978 when the TNRSF project was initiated. The third model scenario represents the case in which the TNRSF project was not initiated in 1978 (without the TNRSF).

2.3. Air−Canopy−Soil Exchange and Deposition Processes. The air−canopy−soil exchange processes for PAHs in CanMETOP were simulated using a fugacity-based multicompartmental mass balance model.[41] The mass balance equation for the forest canopy compartment is

$$\frac{d(V_F \cdot Z_F \cdot f_F)}{dt} = D_{AF} \cdot f_A - (D_{RF} + D_{FA} + D_{FB}) \cdot f_F \quad (1)$$

where V_F and Z_F are the volume and the fugacity capacity of the foliage compartment (m^3 and mol m^{-3} Pa^{-1}), respectively, and f_F and f_A are the fugacities in foliage and atmosphere (Pa), respectively. Four D values (mol h^{-1} Pa^{-1}) representing processes in the forest canopy compartment were taken into consideration: foliar uptake of a chemical from the atmosphere D_{AF}, loss of the chemical from foliage to the atmosphere (e.g., via evaporation) D_{FA}, transfer of the chemical from foliage to soil D_{FB}, and degradation of the chemical in the foliage compartment D_{RF}. Foliar uptake from the atmosphere can occur via gaseous uptake, dry particle deposition, and wet deposition. The volatilization of the chemical from the foliage is treated as gaseous exchange. The transfer of the chemical from foliage to soil mainly occurs through litterfall. Here the targeted chemicals were considered hydrophobic, hence, the root uptake and transport within the plant are negligible and no uptake of PAHs by soil is considered. Detailed calculations of V_F, Z_F, and D values in eq 1 are presented in Supporting Information (section SI5).

PAHs concentration (C_F) in foliage can be estimated by the fugacity in foliage (f_F)

$$C_F = Z_F \times f_F \quad (2)$$

The air−canopy exchange flux F_F (ng m^{-2} h^{-1}) is expressed as[42]

$$F_F = k_u 2(\mathrm{LAI})\left(C_A - \frac{C_F}{K_{FA}}\right) \quad (3)$$

where k_u is the air−canopy mass transfer coefficient (m h^{-1}), LAI is the leaf area index, C_A is PAHs concentration in air (ng m^{-3}), and K_{FA} is the leaf-air partition coefficient (m^3 of air per g of leaf dw).

The air−soil exchange flux F_g (ng m^{-2} h^{-1}) can be estimated as[43]

$$F_g = \mathrm{MTC}\left(C_A - \frac{C_S \rho_S}{K_{SA}}\right) \quad (4)$$

where C_S is soil concentration (ng kg^{-1}, dry weight), MTC is the overall mass transfer coefficient (cm s^{-1}), ρ_S is the density of the soil solids (kg m^{-3}), and K_{SA} is soil−air partition coefficient. Detailed calculation for k_u, K_{FA}, MTC, and K_{SA} are presented in Supporting Information (section SI5).

A dry deposition scheme for fine ($PM_{2.5}$), coarse ($PM_{2.5-10}$), and giant (PM_{10+}) particles recently developed by Zhang and He[44,45] was adopted to calculate dry deposition velocity of particle-bound PAHs. To avoid overestimation of the selected PAHs dry deposition, particle-bound BaP was assumed to be in the accumulation mode with particle diameters between 0.1 and 2.5 μm,[46] although a mass fraction of 0.3 was used for coarse particles in Zhang et al.[45] The surface roughness length and LAI (leaf area index) data used in the estimation of dry deposition velocities were obtained from Zhang et al.[16] (Figures S5−S7). The meteorological data used in the modeling and computation of the dry deposition velocity include monthly mean surface and skin temperatures, relative humidity, precipitation, surface pressure, and wind. These data were collected from the 1° × 1° latitude/longitude NCEP (National Centers for Environmental Prediction) Final Operational Global Analysis (rda.ucar.edu/datasets/ds083.2/) and then interpolated into the CanMETOP model grids on the spatial resolution of 1/4° × 1/4° latitude/longitude.

3. RESULTS AND DISCUSSION

3.1. Field and Model Evidence. The global distribution of OCs has been shown to be strongly associated with the distribution of SOC.[22,24,47] To examine soil absorption of PAHs in the TNRSF, a field campaign was conducted to measure soil levels of the selected PAHs inside and outside the TNRSF. Compared with bare soil, forest soil with higher organic carbon has a higher absorption of OCs. Figure 1 illustrates sampled soil concentrations of PHE and BaP at the four paired sites (Section 2.1). As shown, the soil levels of PHE and BaP at the four forest sites are higher than those outside the forest, confirming that the TNRSF soil is a potential reservoir of PAHs.

In addition to the absorption of OCs due to high SOC in forest soils, forests increase the surface roughness which could enhance the dry deposition of OCs.[7,21,45] Another pathway of OCs uptake by forest canopy and transfer to soil is litterfall. Thus, the significance of the TNRSF in transferring PAHs from atmosphere to soil can also be demonstrated by comparing air-soil net gaseous exchange, dry particle deposition, and air-canopy net exchange at locations within and outside the TNRSF. To do so, we selected two small areas (squares), each consists of 4 grid points. We then calculated the mean air-soil net gaseous exchange fluxes, dry particle deposition fluxes, and air-canopy exchange fluxes of PHE and BaP in the selected small areas. These two small areas are marked in Figure S1. One area is located in the Central-North region of the TNRSF, and the other is farmland located outside the TNRSF. Since the anthropogenic emissions of PHE and BaP increased markedly after 2000 (Figure S4), it is expected that the PHE and BaP emissions would overwhelm their atmospheric levels and exchange fluxes in the past 20 years. To exclude the effect of the emissions on the spatial distribution and temporal trends of PHE and BaP, we adopted the model Scenario 1 in which the

DOI: 10.1021/acs.est.6b04835
Environ. Sci. Technol. XXXX, XXX, XXX−XXX

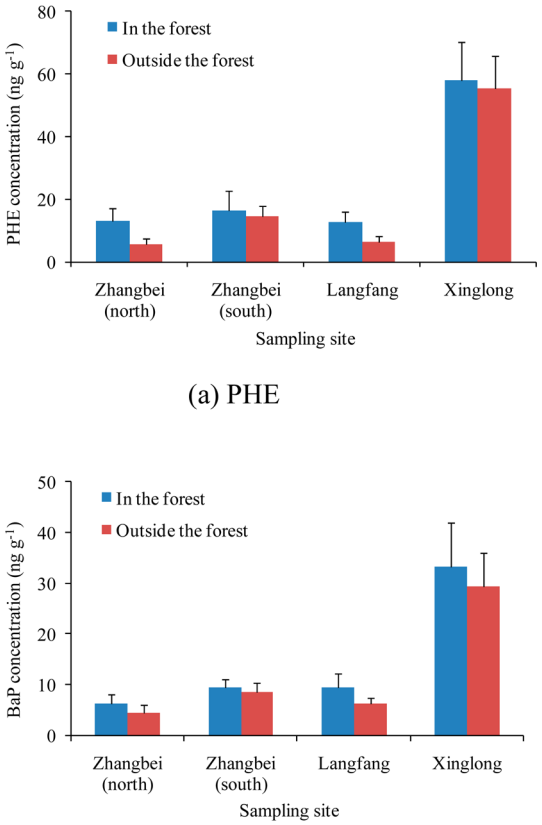

Figure 1. Soil concentration of PHE (a) and BaP (b) inside and outside the forest at four paired sampling sites in the Central-North region of the TNRSF as marked in Figure S2. The error bars (shown as black lines) represent one standard deviation.

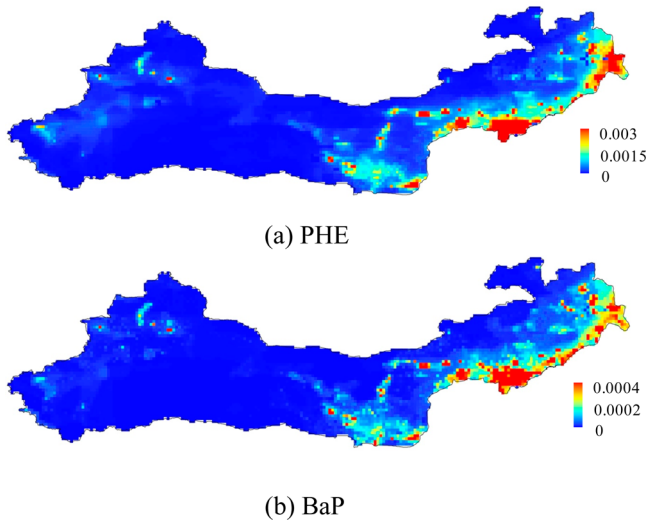

Figure 2. Average net exchange flux (mg m^{-2} d^{-1}) (dry gas-phase deposition + dry particle deposition + wet deposition + uptake of canopy − revitalization from soil − revitalization from canopy) for PHE (a) and BaP (b) over the TNRSF from 1990 to 2010, simulated using annual emissions of PHE and BaP as well as annual LAI and SOC from 1990 to 2010. Positive values of the total net exchange indicate the removal of PAHs from the atmosphere, and negative values indicate the net volatilization from underlying surfaces.

emissions of the two PAHs congeners were not annually altered. The model was then integrated from 1990 to 2010. The results are illustrated in Figure S13. As observed, air-soil net gaseous exchange fluxes, dry particle deposition fluxes, and air-canopy exchange fluxes of PHE and BaP within the TNRSF were a factor of 3−5 greater than those in the area outside the TNRSF. Because of the increase in LAI and SOC in the TNRSF, these fluxes within the TNRSF exhibited statistically significant increasing trends compared with those in the farmland outside the TNRSF where no trends were identified for these fluxes in both PAH congeners.

3.2. Total Removal of PAHs from the Atmosphere by the TNRSF. Figure 2 shows the spatial patterns of modeled averaging net exchange flux (diffusive gas-phase deposition + dry particle deposition + uptake of canopy + wet deposition − volatilization from soil − volatilization from canopy) of PHE and BaP from 1990 to 2010. They were simulated by the model Scenario 2 using the annual PHE and BaP emissions, LAI, and SOC from 1990 to 2010. Positive values of the total net exchange indicate the removal of PAHs from the atmosphere, and negative values indicate elevated PAHs in the air. Overall, greater removal of PAHs can be observed in the Northwest and the Central-North regions of the TNRSF, the part of Shaanxi and Ningxia province, and the west of Xinjiang province. The largest removal of PHE and BaP can be found in northeast Hebei, northern Liaoning, and central Heilongjiang provinces due to higher PAH emissions in these regions (Figure S12). The steel industries in China, as major sources of PAHs, are mainly located in Hebei and Liaoning provinces. The crude steel industries in these two provinces accounted for 42% of the national total crude steel production in 2010.[48]

We further estimated the annual total removal of PHE and BaP from the atmosphere by diffusive gas-phase deposition, dry particle depositions, uptake from canopy, and wet deposition in the TNRSF. The results show that the total removal of PHE from the atmosphere increased from 36.4 tons in 1990 to 76.8 tons in 2010, with an annual rate increase of 5.6% yr^{-1} (Table 1). The fraction of the atmospheric removal for PHE, calculated as the ratio of total removals (diffusive gas-phase deposition from air to soil + dry particle deposition + uptake from canopy + wet deposition) to total emissions (primary emission + the secondary emission due to revolatilization from soil and canopy), was approximately 2.7% in 1990 and 3.0% in 2010, benefiting from continuous expansion of the TNRSF over this period of time. The diffusive gas-phase deposition contributed to the largest portion of the PHE removal (1.9%) from the atmosphere, followed by particle-bound dry deposition (0.5%), air-canopy uptake from canopy (0.4%), and wet deposition (0.1%) in 2010. The total removal of BaP from the atmosphere increased from 2.2 tosn in 1990 to 4.5 tons in 2010, with an annual rate increase of 5.2% yr^{-1}. The percentage of BaP removal was approximately 1.3% in 1990 and 1.5% in 2010. Since BaP is mostly particle-bound, the dry particle deposition made the largest contribution to the removal of BaP from the atmosphere (0.6%), followed by diffusive gas-phase deposition (0.5%), air-canopy uptake (0.3%), and wet deposition (0.1%). The air-soil and air-canopy exchange played a slightly more important role in the removal of PHE than BaP. The modeling results also revealed that the accumulation of the two PAH congeners in plant canopy was merely 6.3% for PHE and 8.6% for BaP in the TNRSF in 2010. A large portion of PHE and BaP absorbed by the forest canopy could be subsequently transferred to the soil by falling litters and throughfall. It can

DOI: 10.1021/acs.est.6b04835
Environ. Sci. Technol. XXXX, XXX, XXX−XXX

Table 1. Removal of PAHs from the Atmosphere by TNRSF from 1990 to 2010[a]

			1990	1995	2000	2005	2010
PHE	emission (tons)		1309 ± 393	1315 ± 396	1262 ± 379	1792 ± 538	2502 ± 751
	volatilization (tons)	from soil	14.16 ± 4.81	15.98 ± 5.43	14.07 ± 4.78	20.38 ± 6.93	29.38 ± 9.98
		from canopy	1.34 ± 0.38	1.62 ± 0.45	1.30 ± 0.36	1.95 ± 0.55	3.18 ± 0.89
		total	15.50 ± 5.19	17.60 ± 5.89	15.37 ± 5.15	22.33 ± 7.48	33.43 ± 11.17
	transportation (tons)	dry particle-phase deposition	7.37 ± 2.21	7.86 ± 2.36	7.57 ± 2.27	10.27 ± 3.08	15.17 ± 4.56
		wet deposition	0.92 ± 0.24	1.08 ± 0.28	0.81 ± 0.21	1.47 ± 0.38	2.08 ± 0.54
		soil absorption	23.59 ± 8.02	26.63 ± 9.06	23.45 ± 7.97	33.97 ± 11.55	48.97 ± 16.65
		uptake from canopy	4.47 ± 1.25	5.40 ± 1.51	4.33 ± 1.21	6.51 ± 1.82	10.59 ± 2.96
		litterfall	2.95 ± 1.12	3.55 ± 1.35	2.84 ± 1.08	4.29 ± 1.63	6.94 ± 2.64
		total removal	36.36 ± 11.72	40.98 ± 13.21	36.15 ± 11.66	52.21 ± 16.83	76.82 ± 24.71
	fraction of removal (%)		2.74	3.09	2.83	2.88	3.03
BaP	emission (tons)		157 ± 47	145 ± 43	149 ± 45	216 ± 65	289 ± 87
	volatilization (tons)	from soil	0.08 ± 0.03	0.08 ± 0.03	0.07 ± 0.03	0.1 ± 0.04	0.14 ± 0.05
		from canopy	0.02 ± 0.005	0.03 ± 0.01	0.02 ± 0.01	0.04 ± 0.01	0.07 ± 0.02
		total	0.10 ± 0.03	0.11 ± 0.03	0.10 ± 0.03	0.14 ± 0.05	0.22 ± 0.07
	transportation (tons)	dry particle-phase deposition	0.92 ± 0.28	1.12 ± 0.34	1.00 ± 0.30	1.41 ± 0.42	1.66 ± 0.50
		wet deposition	0.16 ± 0.04	0.17 ± 0.05	0.14 ± 0.04	0.22 ± 0.06	0.31 ± 0.08.
		soil absorption	0.83 ± 0.28	0.94 ± 0.32	0.83 ± 0.28	1.22 ± 0.41	1.59 ± 0.54
		uptake from canopy	0.29 ± 0.08	0.40 ± 0.11	0.31 ± 0.09	0.68 ± 0.19	0.96 ± 0.27
		litterfall	0.25 ± 0.1	0.34 ± 0.13	0.23 ± 0.09	0.60 ± 0.23	0.81 ± 0.31
		total	2.20 ± 0.68	2.64 ± 0.81	2.28 ± 0.70	3.52 ± 1.08	4.52 ± 1.39
	fraction of removal (%)		1.40	1.65	1.53	1.63	1.56

[a]The ± value represents 1 standard deviation derived from the confidence factors Cf_{out} in the uncertainty analysis (eq 18 of SI). The fractions of atmospheric removal were calculated as the ratio of total removals (dry particle deposition + wet deposition + soil absorption + uptake from canopy) to total emissions (primary emission + the secondary emission due to revolatilization from soil and canopy).

also be observed from Table 1 that the revolatilization of PHE from canopy and soil accounted for approximately 43% of the total removal by air−canopy and air−soil exchange, which may offset the removal of PHE from the atmosphere. The upward flux of PHE was higher than that of BaP (5%) because of its lower log K_{OA} (7.64 at 298 K) compared with BaP (11.48 at 298 K).[49]

Simonich and Hites have estimated that 44% of PAH emissions in the northeastern United States deposited to vegetations, the majority of which are forests;[29] however, this estimate was subsequently revised to 4%.[50] This study yields a 1−4% removal of PHE and BaP from the atmosphere by the TNRSF after their release from sources in northern China and subsequent transport to the TNRSF, which is somewhat consistent with the estimate by Wagrowski et al.[50] It should be noted that the TNRSF also includes other land use types, such as urban and built-up lands, barren or sparsely vegetated lands, shrubs, and Gobi, which still occupy a large area of the Northwest region of the TNRSF. In addition, this study used the most recently updated modules of dry particle deposition velocities for PAHs which were derived based on data from field measurements.[45] This enhances our confidence in the estimation of atmospheric particle deposition by the TNRSF.

3.3. Effect of the TNRSF on the Atmospheric Removal of PAHs. We performed the model Scenario 1 simulation with the fixed emission of PHE and BaP to highlight the contribution of the changes in the artificial land-use by the TNRSF on the removal of PAHs from atmosphere. In this case, the forest expansion in the TNRSF were featured by annual variation of the LAI and SOC from 1990 to 2010. Figure S14 illustrates the trend of PHE and BaP fluxes due to air-soil net gas exchange flux (diffusive gas-phase deposition from air to soil *minus* volatilization from soil to air), dry particle deposition, air-canopy net gas exchange flux (uptake from air to canopy *minus* volatilization from canopy to soil), and litterfall averaged over the TNRSF. Wet deposition fluxes are not illustrated here because precipitation is not directly linked with the TNRSF. As shown in Figure S14, all 4 category fluxes displayed an increasing trend from 1990 to 2010, supporting plausible influences of the extension of vegetation coverage across the TNRSF on the removal of PAHs from the atmosphere. Due to its hydrophobic nature, sorption to the soil organic carbon fraction is the main partitioning mechanism of POPs to soil. The increasing vegetation coverage in the TNRSF led to the increase of SOC which in turn increased air-soil net gas exchange fluxes for both PAHs congeners. Because the air-canopy exchange fluxes of PHE and BaP were positively correlated with LAI, increasing vegetation coverage with the development of the TNRSF in the past two decades resulted in increasing PAHs uptake by the canopy and deposition by litterfall. It is worth noting that the estimated fluxes in model Scenario 2 declined from 2007, as shown in Figure S14. This was due to the mortality of trees in the Central-North region of the TNRSF since 2007.[51,52] Approximately 10−50% of trees planted since the late 1970s were reported dead in this region since 2007, causing a considerable decrease of the forest coverage that in turn subsequently led to the decrease of PHE and BaP uptake and exchange fluxes in the TNRSF.

The long-term trends of the net exchange flux of PHE and BaP induced by the development of the TNRSF were estimated by linear regressions of the gridded daily average net exchange flux of PHE and BaP derived from model Scenario 1 against their time sequence of 1990 through 2010. The gridded slopes (trends) of the linear regressions of daily average net exchange flux are shown in Figure 3. The nonparametric Mann-Kendall statistical test (Z) for the daily average net exchange fluxes of PHE and BaP from 1990 to 2010 was performed to examine the statistical significance of the estimated trends (black cross in

DOI: 10.1021/acs.est.6b04835
Environ. Sci. Technol. XXXX, XXX, XXX−XXX

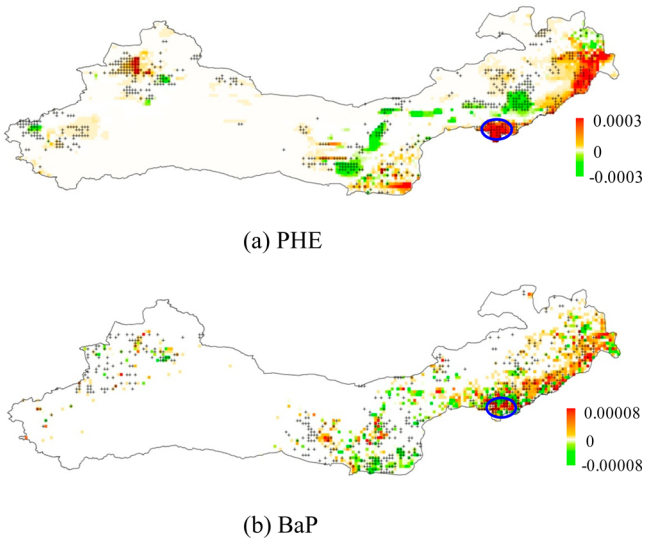

Figure 3. Slope (trend) of linear regression relationship between annually averaged daily net exchange flux (ng m^{-2} d^{-1}) of PHE (a) and BaP (b) and the time sequence from 1990 to 2010 across the TNRSF using the fixed annual PHE and BaP emissions averaged over 1990 to 2010 and annual LAI and SOC for the same time period (model Scenario 1). The areas filled with black crosses indicate the regions where the trend is statistically significant at the 95% confidence in terms of the Mann–Kendall statistical test ($|Z| > 1.96$). The blue circle denotes the regions where 12 grid points were selected to project air–soil net exchange flux and air-canopy net exchange flux in this area until 2050. The positive values indicate an increasing trend of net exchange fluxes from 1990 to 2010, and vice versa.

Figure 3). Since the start of the TNRSF program in the later 1970s, the forest coverage in this region reached 12.4% in 2010,[10] which increased markedly LAI and SOC in this region. Figure S15 shows the slopes (trends) of linear regression relationships between annual mean SOC and the time sequence from 1990 to 2010 across the TNRSF. The positive trends of LAI and SOC can be observed in eastern Qinghai province of the Northwest, Central-North region, and most of the Northeast region of the TNRSF. These regions virtually achieved the largest success in terms of tree seeding and planting over the last several decades.[53] Accordingly, the significantly increasing trend of the net exchange flux of PHE and BaP can also be identified in those areas with increasing LAI and SOC in the Northeast, Central-North, and the west of Xinjiang province of the TNRSF (Figure 3). Greater values of positive trends of the net exchange flux of PHE can be observed in northeastern Hebei province, central Liaoning, and eastern Heilongjiang, northern Shaanxi, and western Xinjiang provinces. The net exchange flux of PHE was mainly from air-soil net exchange whereas the dry particle deposition made the largest contribution to the net exchange flux for BaP. The higher positive trends of the net exchange fluxes of BaP are also visible in those areas with greater emission and roughness lengths across the TNRSF, such as eastern Hebei, central Liaoning and Jilin, eastern Heilongjiang, part of Ninxia and Qinghai, and eastern Gansu provinces. As mentioned, the roughness lengths in the present study were derived from the NDVI.[16] Hence, the consistence of the dry particle deposition fluxes with the roughness length imply that greater removal of BaP in the TNRSF was attributed, to some extent, to the areas with faster growing vegetation coverage. Relatively large values and increasing trend of the LAIs can be found in the border region between Shaanxi and Shanxi provinces (Figure S16); however, the net exchange flux of BaP exhibited negative trends in this region. This is largely attributed to the relatively lower BaP emissions in this region (Figure S3).

3.4. Projected Atmospheric Removal of PAHs with and without TNRSF. Further insight on the significance of the TNRSF in the removal of the selected PAHs can be gained by comparing modeled fluxes between model Scenarios 2 and 3. As mentioned, Scenario 3 virtually postulated no TNRSF by using the fixed LAI and SOC in 1978 over the TNRSF region, whereas Scenario 2 took into account the annual changes in the SOC and LAI over the TNRSF. Both scenarios incorporated annually varying emissions of 1990 through 2010 over northern China. The fractions of atmospheric removal, defined in section 3.2, were also estimated for the results of Scenario 3 and compared with those from Scenario 2 (Figure 4). The

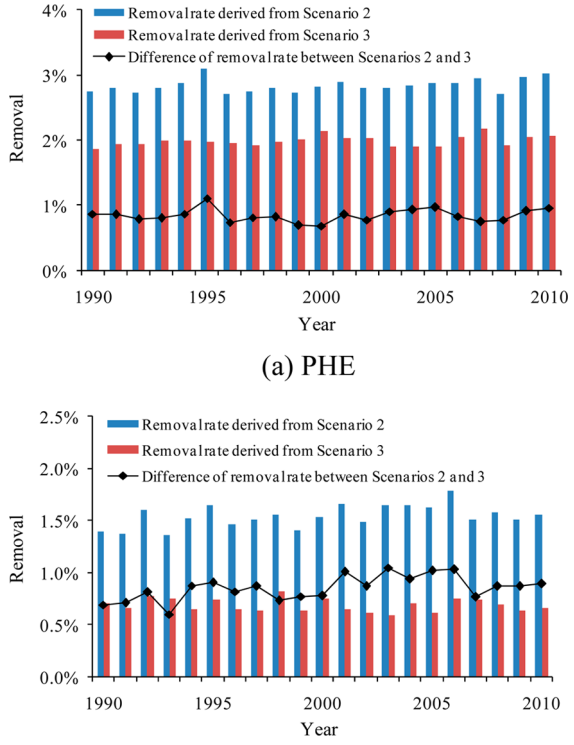

Figure 4. Comparisons between annual average uptake fraction for PHE (a) and BaP (b) from 1990 to 2010 derived from Scenario 2 (annual PHE and BaP emissions from 1990 to 2010 and annual LAI and SOC for the same time period) and Scenario 3 (annual PHE and BaP emissions averaged over 1990 to 2010 and fixed LAI and SOC in 1978). The solid black lines represent the differences of the annual mean uptake fraction by the TNRSF between model scenarios 2 and 3.

multiyear mean removal fractions in Scenario 2 were 2.8% for PHE and 1.5% for BaP, whereas those in Scenario 3 were approximately 2% for PHE and 0.7% for BaP. This suggests that the TNRSF has enhanced the atmospheric removal by 29% for PHE and 53% for BaP. In particular, due to the greater increasing trend of LAI and SOC in the Central-North region (Figures S15 and S16), the artificial forest in this region has enhanced the atmospheric removal by 43% for PHE and 72% for BaP. For BaP, the differences of the removal fractions with and without the TNRSF exhibited an increasing trend (Figure 4b, solid black line), confirming the increasing contribution of the TNRSF to the atmospheric removal of this most toxic PAH congener. These results also imply that, although the TNRSF

DOI: 10.1021/acs.est.6b04835
Environ. Sci. Technol. XXXX, XXX, XXX–XXX

merely removes 1−4% of PHE and BaP from the atmosphere, the depletion of PAHs in the atmosphere would be much lower without the presence of the TNRSF.

Since the TNRSF program will continue until 2050, the LAI and SOC across the TNRSF would very likely increase in coming years until its biomass reaches a steady state. To project potential changes in PAHs exchange fluxes in the future resulting from continued increases of LAI and SOC over the TNRSF, we estimated the linear regressions between PAHs fluxes and the SOC and LAI across the TNRSF using the linear models of LAI and SOC as shown in Figures S15 and S16. In this way, we extended the modeled air-soil net exchange flux and air-canopy net exchange fluxes to 2050. Figure S17 shows projected air-soil and air-canopy net exchange fluxes in a small area marked by the blue solid line in Figure 3 where the LAI and SOC exhibited statistically significant increasing trends ($r > 0.8$, $p < 0.01$). As observed, the air-soil net exchange fluxes of PHE and BaP will reach 0.03 and 0.002 mg m^2 d^{-1}, respectively, by 2050, and the air-canopy net exchange fluxes of the two species will reach 0.02 and 0.001 mg m^2 d^{-1}, respectively. This indicates that the projected air-soil net exchange flux and the air-canopy net exchange fluxes would increase by 1.8 and 1.9 times for PHE, and 1.5 and 1.8 times for BaP from 1990 to 2050.

Compared with natural forests under a steady-state, we have shown that, as the largest artificial forest in human history, the TNRSF plays an increasingly significant role in the atmospheric removal of OCs in northern China, and the assessment of its development and evolution over the past several decades has contributed to understanding of the effect of large-scale land-use change on air quality and the biogeochemical cycling of OCs. Such an assessment is often required by policy makers and the public. Since the TNRSF will extend until 2050, it is expected that this program will make increasing contributions to the improvement of air quality in northern China.

■ ASSOCIATED CONTENT

Supporting Information

The Supporting Information is available free of charge on the ACS Publications website at DOI: 10.1021/acs.est.6b04835.

Study area, in situ field measurement, description of the sampling site, sample collection, chemical analysis, quality control, CanMETOP atmospheric transport model, soil organic carbon (SOC), air−canopy−soil exchange processes, model evaluation, uncertainty analysis, PAH concentration in various environmental medias in 2010, effects of the TNRSF on the removal of PAHs, the Three Northern Regions Shelter Forest (TNRSF) in Northern China, sampling sites (red triangle) in the field campaign, atmospheric PAHs emissions (1×10^6 kg) in northern China from 1990 to 2010, spatial of atmospheric emission of PAHs, spatial distribution of surface roughness length in the TNRSF in 2010, spatially averaged LAI and SOC across the TNRSF from 1990 to 2010, spatial distribution of LAI in the TNRSF in 2010, spatial distribution of SOC in the TNRSF in 2010, vertical distribution of organic carbon content in the soil profile, comparison between modeled and sampled air concentrations of PHE and BaP across the TNRSF, comparison between modeled and sampled soil concentrations of PHE and BaP across S3 TNRSF, spatial distributions of the seasonal mean PAHs in various environmental media, different exchange fluxes of PHE and BaP over the two small areas within and outside the TNRSF in Central-North China, spatially averaged daily fluxes of PHE and BaP from different exchange and uptake processes over the TNRSF from 1990 to 2010 derived from scenario 1, slope of linear regression relationship between the annual mean SOC and the time sequence from 1990 to 2010 across the TNRSF, slope of linear regression relationship between the annual mean LAI and the time sequence from 1990 to 2010 across the TNRSF, forecasting net air−soil exchange flux and net air−canopy flux for PHE and BaP from 1990 to 2050, vegetation types and latitude/longitude of sampling sites inside and outside of forest, physicochemical properties of PHE and BaP, input parameters used in air-forest canopy-forest soil exchange processes modeling, comparison of the modeled and measured air concentrations of PHE and BaP, comparison between modeled and measured PHE and BaP concentrations in soil, measured PHE and BaP concentrations in needles in some regions in China (PDF)

■ AUTHOR INFORMATION

Corresponding Author

*E-mail: jianminma@lzu.edu.cn.

ORCID

Jianmin Ma: 0000-0002-6593-570X

Notes

The authors declare no competing financial interest.

■ ACKNOWLEDGMENTS

This research was supported by the National Natural Science Foundation of China through grants 41503089, 41371478, and 41371453, as well as the Natural Science Foundation of Gansu Province of China (1506RJZA212).

■ REFERENCES

(1) Dutchak, S., Zuber, A., Eds. Task Force on Hemispheric Transport of Air Pollution. *Hemispheric Transport of Air Pollution 2010—Part C: Persistent Organic Pollutants*; United Nations Press: New York, 2010.

(2) Macdonald, R. W.; Mackay, D.; Li, Y. F.; Hickie, B. How will global climate change affect risks from long-range transport of persistent organic pollutants? *Hum. Ecol. Risk Assess.* **2003**, *9*, 643−660.

(3) Armitage, J. M.; Wania, F. Exploring the potential influence of climate change and particulate organic carbon scenarios on the fate of neutral organic contaminants in the Arctic environment. *Environ. Sci.-Proc. Imp.* **2013**, *15*, 2263−2272.

(4) Kallenborn, R.; Halsall, C.; Dellong, M.; Carlsson, P. The influence of climate change on the global distribution and fate processes of anthropogenic persistent organic pollutants. *J. Environ. Monit.* **2012**, *14*, 2854−2869.

(5) Gouin, T.; Armitage, J. M.; Cousins, I. T.; Muir, D. C. G.; Ng, C. A.; Reid, L.; Tao, S. Influence of global climate change on chemical fate and bioaccumulation: The role of multimedia models. *Environ. Toxicol. Chem.* **2013**, *32*, 20−31.

(6) Ma, J.; Hung, H.; Macdonald, R. W. The influence of global climate change on the environmental fate of persistent organic pollutants: A review with emphasis on the Northern Hemisphere and the Arctic as a receptor. *Glob. Plane. Chan.* **2016**, *146*, 89−108.

(7) Komprda, J.; Komprdova, K.; Sanka, M.; Mozny, M.; Nizzetto, L. Influence of Climate and Land Use Change on Spatially Resolved

DOI: 10.1021/acs.est.6b04835
Environ. Sci. Technol. XXXX, XXX, XXX−XXX

Volatilization of Persistent Organic Pollutants (POPs) from Background Soils. *Environ. Sci. Technol.* **2013**, *47*, 7052−7059.
(8) Wu, Y.; Zeng, Y.; Wu, B. F. Retrieval and analysis of vegetation cover in the Three-North Regions of China based on MODIS data. *Chin. J. Ecol.* **2009**, *28*, 1712−1718.
(9) Wang, Q.; Zhang, B.; Dai, S. P.; Zou, Y.; Ma, Z. H.; Zhang, Y. N. Dynamic changes in vegetation coverage in the Three Northern Regions Shelter Forest program based on GIMMS AVHRR NDVI. *Resour. Sci.* **2011**, *33*, 1613−1620.
(10) Central Government of China. Forest Cover Area From Artifcial Afforestation in the Three Northern Regions Shelter Forest Regions, 2012. Available at: http://www.gov.cn/jrzg/2012-08/27/content_2211594.htm.
(11) Gregory, N. G. The role of shelterbelts in protecting livestock: A review. *N. Z. J. Agric. Res.* **1995**, *38*, 423−450.
(12) Liu, Y. Q.; Stanturf, J.; Lu, H. Q. Modeling the Potential of the Northern China Forest Shelterbelt in Improving Hydroclimate Conditions. *J. Am. Water Resour. Assoc.* **2008**, *44*, 1176−1192.
(13) Wiseman, G.; Kort, J.; Walker, D. Quantification of shelterbelt characteristics using high-resolution imagery. *Agric., Ecosyst. Environ.* **2009**, *131*, 111−117.
(14) An, S.; Mentler, A.; Blum, E. H.; et al. Soil aggregation, aggregate stability, organic carbon and nitrogen in different soil aggregate fractions under forest and shrub vegetation on the Loess Plateau, China. *Catena* **2010**, *81*, 226−233.
(15) Wang, X.; Zhang, C.; Hasi, E.; Dong, Z. Has the Three Norths Forest Shelterbelt Program solved the desertification and dust storm problems in arid and semiarid China? *J. Arid Environ.* **2010**, *74*, 13−22.
(16) Zhang, X.; Huang, T.; Zhang, L.; Gao, H.; Shen, Y.; Ma, J. Trends of deposition fluxes and loadings of sulfur dioxide and nitrogen oxides in the artificial Three Northern Regions Shelter Forest across northern China. *Environ. Pollut.* **2015**, *207*, 238−247.
(17) Nizzetto, L.; Macleod, M.; Borga, K.; Cabrerizo, A.; Dachs, J.; Guardo, A. D.; Ghirardello, D.; Hansen, K. M.; Jarvis, A.; Lindroth, A.; Ludwig, B.; Monteith, D.; Perlinger, J.; Scheringer, M.; Schwendenmann, L.; Semple, K. T.; et al. Past, Present, and Future Controls on Levels of Persistent Organic Pollutants in the Global Environment. *Environ. Sci. Technol.* **2010**, *44*, 6526−6531.
(18) Horstmann, M.; McLachlan, M. S. Atmospheric deposition of semivolatile organic compounds to two forest canopies. *Atmos. Environ.* **1998**, *32*, 1799−1809.
(19) Nizzetto, L.; Cassani, C.; Di Guardo, A. Deposition of PCBs in mountains: The forest filter effect of different forest ecosystem types. *Ecotoxicol. Environ. Saf.* **2006**, *63*, 75−83.
(20) Brorström-Lundén, L. E.; Löfgren, C. Atmospheric fluxes of persistent semivolatile organic pollutants to a forest ecological system at the Swedish west coast and accumulation in spruce needles. *Environ. Pollut.* **1998**, *102*, 139−149.
(21) Su, Y.; Wania, F.; Harner, T.; Lei, Y. D. Deposition of polybrominated diphenyl ethers, polychlorinated biphenyls, and polycyclic aromatic hydrocarbons to a boreal deciduous forest. *Environ. Sci. Technol.* **2007**, *41*, 534−540.
(22) Meijer, S. N.; Ockenden, W. A.; Sweetman, A.; Breivik, K.; Grimalt, J. O.; Jones, K. C. Global distribution and budget of PCBs and HCH in background surface soils: implications for sources and environmental processes. *Environ. Sci. Technol.* **2003**, *37*, 667−672.
(23) Wania, F.; Su, Y. Quantifying the global fractionation of polychlorinated biphenyls. *Ambio* **2004**, *33*, 161−168.
(24) Zheng, Q.; Nizzetto, L.; Mulder, M. D.; Sáňka, O.; Lammel, G.; Li, J.; Bing, H.; Liu, X.; Jiang, Y.; Luo, C.; Zhang, G. Does an analysis of polychlorinated biphenyl (PCB) distribution in mountain soils across China reveal a latitudinal fractionation paradox? *Environ. Pollut.* **2014**, *195*, 115−122.
(25) Howsam, M.; Jones, K. C.; Ineson, P. Dynamics of PAH deposition, cycling and storage in a mixed-deciduous (Quercusfraxinus) woodland ecosystem. *Environ. Pollut.* **2001**, *113*, 163−176.
(26) Howsam, M.; Jones, K. C.; Ineson, P. PAHs associated with the leaves of three deciduous tree species-II: Uptake during a growing season. *Chemosphere* **2001**, *44*, 155−164.
(27) Matzner, E. Annual rates of deposition of polycyclic aromatic hydrocarbons in different forest ecosystems. *Water, Air, Soil Pollut.* **1984**, *21*, 425−434.
(28) McLachlan, M. S.; Horstmann, M. Forests as filters of airborne organic pollutants: a model. *Environ. Sci. Technol.* **1998**, *32*, 413−420.
(29) Simonich, S. L.; Hites, R. A. Importance of vegetation in removing polycyclic aromatic hydrocarbons from the atmosphere. *Nature* **1994**, *370*, 49−51.
(30) Hagenmaier, H.; Krauβ, H. B. Attempts to balance transport and fate of polychlorinated dibenzo-p-dioxins and dibenzofurans for Baden-Württemberg. *Organohalogen Compd.* **1993**, *13*, 81−84.
(31) Meijer, S. N.; Steinnes, E.; Ockenden, W. A.; Jones, K. C. Influence of environmental variables on the spatial distribution of PCBs in Norwegian and U.K. soils: implications for global cycling. *Environ. Sci. Technol.* **2002**, *36*, 2146−2153.
(32) Sanderson, M. G.; Jones, C. D.; Collins, W. J.; Johnson, C. E.; Derwent, R. G. Effect of climate change in isoprene emissions and surface ozone levels. *Geophys. Res. Lett.* **2003**, *30*, 1936.
(33) Fang, J. Y.; Chen, A. P.; Peng, C. H.; Zhao, S. Q.; Ci, L. J. Changes in forest biomass carbon storage in China between 1949 and 1998. *Science* **2001**, *292*, 2320−2322.
(34) Tan, K.; Piao, S.; Peng, C.; Fang, J. Satellite-based estimation of biomass carbon stocks for northeast China's forests between 1982 and 1999. *For. Ecol. Manage.* **2007**, *240*, 114−121.
(35) Zhang, Y.; Wang, X.; Qin, S. Carbon stocks and dynamics in the three-north protection forest program, China. *Austrian J. For. Sci.* **2013**, *130*, 25−43.
(36) Liu, W.; Zhu, J.; Jia, Q.; Zheng, X.; Li, J.; Lou, X.; Hu, L. Carbon Sequestration Effects of Shrublands in Three-North Shelterbelt Forest Region, China. *Chin. Geogra. Sci.* **2014**, *24*, 444−453.
(37) Ma, J.; Daggupaty, S.; Harner, T.; Li, Y. Impacts of lindane usage in the Canadian prairies on the Great Lakes ecosystem. 1. Coupled atmospheric transport model and modeled concentrations in air and soil. *Environ. Sci. Technol.* **2003**, *37*, 3774−3781.
(38) Ma, J.; Venkatesh, S.; Li, Y.-F.; Daggupaty, S. M. Tracking toxaphene in the North American Great Lakes basin-1. Impact of toxaphene residues in the U.S. soils. *Environ. Sci. Technol.* **2005**, *39*, 8123−8131.
(39) Zhang, Y.; Tao, S. Global atmospheric emission inventory of polycyclic aromatic hydrocarbons (PAHs) for 2004. *Atmos. Environ.* **2009**, *43*, 812−819.
(40) Friedman, C. L.; Pierce, J. R.; Selin, N. E. Assessing the influence of secondary organic versus primary carbonaceous aerosols on long-range atmospheric polycyclic aromatic hydrocarbon transport. *Environ. Sci. Technol.* **2014**, *48*, 3293−3302.
(41) Wania, F.; Persson, J.; Di Guardo, A.; McLachlan, M. S. *CoZMo-POP. A Fugacity-Based Multi-Compartmental Mass Balance Model of the Fate of Persistent Organic Pollutants in the Coastal Zone*, WECC Report 1/2000; WECC Wania Environmental Chemists Corp.: Toronto, Canada, 2000; http://www.utsc.utoronto.ca/labs/wania/wp-content/uploads/sites/4/2014/02/WECC-report-1-2000.pdf.
(42) Nizzetto, L.; Jarvis, A.; Brivio, P. A.; Jones, K. C.; Di Guardo, A. Seasonality of the air-forest canopy exchange of persistent organic pollutants. *Environ. Sci. Technol.* **2008**, *42*, 8778−8783.
(43) Bozlaker, A.; Odabasi, M.; Muezzinoglu, A. Dry deposition and soil−air gas exchange of polychlorinated biphenyls (PCBs) in an industrial area. *Environ. Pollut.* **2008**, *156*, 784−793.
(44) Zhang, L.; He, Z. Technical Note: An empirical algorithm estimating dry deposition velocity of fine, coarse and giant particles. *Atmos. Chem. Phys.* **2014**, *14*, 3729−3737.
(45) Aulinger, A.; Matthias, V.; Quante, M. Introducing a Partitioning Mechanism for PAHs into the Community Multiscale Air Quality Modeling System and Its Application to Simulating the Transport of Benzo(a)pyrene over Europe. *J. Appl. Meteorol. Clim.* **2007**, *46*, 1718−1729.
(46) Zhang, L.; Cheng, I.; Wu, Z.; Harner, T.; Schuster, J.; Charland, J. P.; Muir, D.; Parnis, J. M. Dry deposition of polycyclic aromatic compounds to various land covers in the Athabasca oil sands region. *J. Adv. Model. Earth Syst.* **2015**, *7*, 1339−1350.

DOI: 10.1021/acs.est.6b04835
Environ. Sci. Technol. XXXX, XXX, XXX−XXX

(47) Nam, J. J.; Gustafsson, O.; Kurt-Karakus, P.; Breivik, K.; Steinnes, E.; Jones, K. C. Relationships between organic matter, black carbon and persistent organic pollutants in European background soils: Implications for sources and environmental fate. *Environ. Pollut.* **2008**, *156*, 809−817.
(48) NBSC (National Bureau of Statistics of China). *China Statistical Yearbook 2010*. China Statistics Press: Beijing, 2011.
(49) Mackay, D.; Shiu, W. Y.; Ma, K. C.; Lee, S. C.*Handbook of Physical−Chemical Properties and Environmental Fate for Organic Chemicals*; CRC Press: Boca Raton, 2006.
(50) Wagrowski, D. M.; Hites, R. A. Polycyclic aromatic hydrocarbon accumulation in urban, suburban, and rural vegetation. *Environ. Sci. Technol.* **1997**, *31*, 279−282.
(51) Zhang, Y.; Wang, X.; Qin, S. Carbon stocks and dynamics in the three-north protection forest program, China. *Austrian J. For. Sci.* **2013**, *130*, 25−43.
(52) Tan, M.; Li, X. Does the Green Great Wall effectively decrease dust storm intensity in China? A study based on NOAA NDVI and weather station data. *Land Use Policy* **2015**, *43*, 42−47.
(53) Zhu, J.; Zhou, X.; Hu, J. Thoughts and views about the three-north shelterbelt program. *J. Nat. Resour.* **2004**, *19*, 79−85.

DOI: 10.1021/acs.est.6b04835
Environ. Sci. Technol. XXXX, XXX, XXX−XXX